KIEE International Transactions on EMECS, Vol. 4-B No. 3, pp. 103~107, 2004 **103**

Rotor Loss Analysis of Permanent Magnet High-Speed Machine According to Magnetization Pattern

Han-Wook Cho†, Seok-Myeong Jang*, Sung-Ho Lee, Hyun-Sup Yang*** and Yeon-Ho Jeong******

Abstract - Recently, greater attention has been paid to the high-speed generator for its many merits, such as ease of installation, high efficiency and high power density. However, due to their high fundamental frequency, careful consideration needs to be given to both electromagnetic and mechanical design issues. This paper deals with the comparison of two types of permanent magnet high-speed machines. Specifically, the effect of the permanent magnet magnetization pattern on the rotor losses is investigated. On the basis of analytical field analysis and the 2-D finite element method, this paper predicts the flux harmonics and rotor losses under the no-load condition. It is shown that the Halbach magnetization is superior to parallel magnetization in terms of producing rotor losses.

Keywords: Flux harmonics, Halbach magnetization, high-speed machines, magnetization pattern, rotor losses, flux harmonics.

1. Introduction

Permanent magnet high-speed machines are likely to be a key technology for electric drives and motion control systems for many applications, since they are conductive to high efficiency, high power density, small size and low weight. Recently, distributed power generation has taken pressure off electric transmission infrastructure with several benefits, such as low emissions, fuel flexibility and high efficiency. For small gas turbines, it is advantageous to omit the gear box that normally reduces the shaft speed for driving conventional low speed generators [1, 2].

For high-speed machines driven by micro turbines, the rotor speed is above 30 000-r/min and exceeds 10 000-r/min. The frequency of flux variation in the stator teeth and core can be more than 1 kHz.

In high-speed machines, the permanent magnets are often contained within a retaining sleeve. However, the sleeve and the magnets are exposed to high order flux harmonics, which cause parasitic eddy current losses. Rotor losses of high-speed machines are of great importance especially in high-speed applications, because losses heat the rotor, which is often a very compact construction and thereby difficult to cool. This causes a danger of demagnetization of the NdFeB permanent magnets. Therefore, special attention should be paid to the prediction of the rotor losses [3].

This paper is concerned with the comparison of rotor losses in two types of permanent magnet high-speed machines that are caused by permeance variation due to stator slotting. First, the flux harmonics are determined by double Fourier analysis of the normal flux density data over the rotor surface. And then, the rectilinear model is used to calculate rotor losses in permanent magnet machines. Finally, this paper describes the influence of magnetization pattern on the rotor losses of permanent magnet high-speed machines. The loss is calculated in two

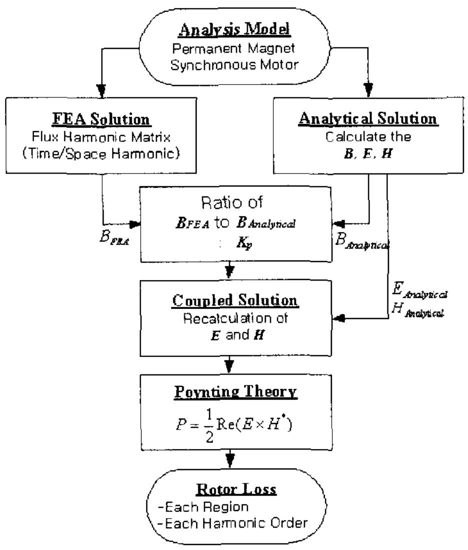

Fig. 1 Flow chart of rotor loss calculation.

† Corresponding Author: Dept of Electrical Engineering, Chungnam National University, Daejeon, Korea. (hwcho@cnu.ac.kr)

* Dept of Electrical Engineering, Chungnam National University, Daejeon, Korea. (smjang@cnu.ac.kr)

** LG Digital Appliance Lab. Seoul, Korea. (iemechas@lge.com)

*** SAMSUNG TECHWIN Co., LTD. Changwon-si, Korea. (hyunsup.yang@samsung.com)

**** Korea Electrotechnology Research Institute, Mechatronics Research Group, Korea. (yhjeong@keri.re.kr)

Received December 23, 2003 ; Accepted July 30, 2004

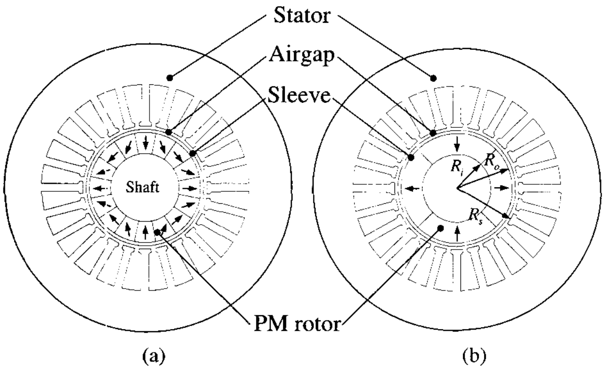

Fig. 2 4-pole, 3-phase permanent magnet high-speed machine topology with (a) Halbach magnetized rotor and (b) parallel magnetized rotor.

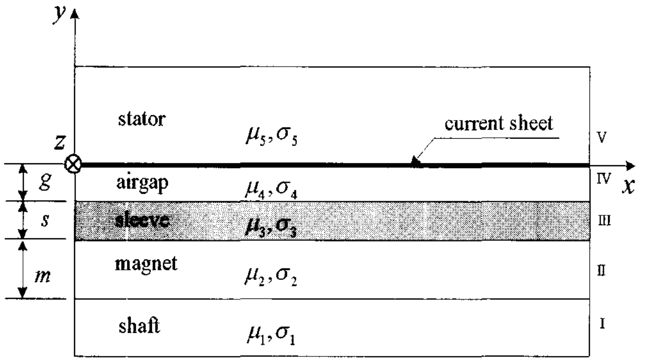

Fig. 3 Simplified rectilinear model.

steps: 1) evaluation of flux traveling waves at the surface of the sleeve, 2) calculation of eddy current loss in the rotor using the current sheet model. These two steps are described in more detail in [5] and [6]. Fig. 1 shows the flow chart of rotor loss calculation.

2. Magnetic Field Analysis

2.1 Analysis Model

Fig. 2 displays a 4-pole, 3-phase high-speed permanent magnet machine with (a) multi-pole Halbach magnetized rotor and (b) parallel magnetized rotor. The topologies were designed as a 5-kW high-speed permanent magnet motor/generator with the rated speed of 40,000-r/min. In order to obtain an analytical solution of the permanent magnet machine, a 2-D rectilinear current sheet model was used and is represented in Fig. 3. The amplitude of the current sheet is chosen to produce the same normal flux density on the surface of the rotor pole-face as does the corresponding harmonic, neglecting the rotor eddy currents caused by relative motion between wave and rotor. Harmonic flux density on the rotor surface has been estimated using conformal mapping techniques [4].

2.2 Evaluation of Flux Harmonics

A total of 15 finite element magneto static models of the machine for different rotor positions are solved. The normal flux density is evaluated over the surface of the sleeve from each solution and data from all solutions are arranged in a 2-dimensional matrix [4]. Fig. 4 shows the normal flux density distribution for the Halbach magnetized rotor at the initial position. Fig. 5 displays the space distribution of normal flux density required to obtain the space and time harmonic distribution at different periods. The figures are made of 15 curves. Using the discrete Fourier transform, the amplitudes of flux density of the traveling harmonics are analyzed.

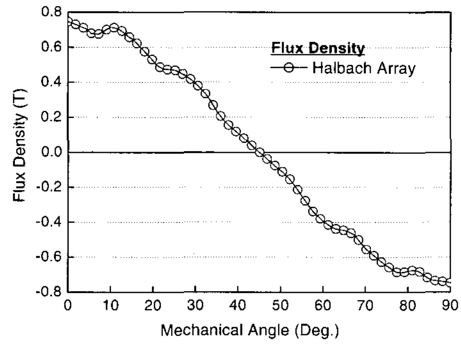

Fig. 4 Space distribution of the normal flux density over the sleeve surface of the Halbach magnetized rotor. (Initial Position)

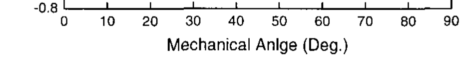

Fig. 5 Space distribution of the normal flux density over the sleeve surface of the Halbach magnetized rotor. (15-data according to rotor angular position)

Table 1 Flux Harmonics of Halbach Magnetization

Space Order	Time Order		
	0	12	24
1	0.727939	0.000058	0.000144
3	0.001209	0.000154	0.000151
11	0.000259	0.016731	0.000070
13	0.000304	0.016040	0.000078
23	0.000050	0.000245	0.004791
25	0.001155	0.000208	0.003922

Table 1 indicates the most significant time and space flux harmonics of the Halbach magnetized model under the no-load condition. All harmonics are backward rotating and space even order harmonics are absent, because of the presence of odd symmetry in the flux space distribution. The number of slots per pole for analysis model is 6. Therefore, the rotor significant harmonics analytical method have a time order of 12th, 24th,... with space order of 11th and 13th, 23th and 25th, ... These harmonics are produced due to interaction of the rotor fundamental harmonic with airgap permeance harmonics [6].

Fig. 6 indicates the normal flux density distribution for the parallel magnetized rotor at the initial position. Fig. 7 shows the space distribution of normal flux density needed to obtain the space and time harmonic distribution at different times. Table 2 shows the most significant time and space flux harmonics of the parallel magnetized model under the no-load condition. All harmonics are backward rotating and space even order harmonics are absent. The rotor significant harmonics analytical method has the time order of 12th, 24th,... with space order of 11th and 13th, 23th and 25th, ...

2.3 Magnetic Field Equation

The governing field equation, in terms of the Coulomb gauge, $\nabla \bullet A = 0$, is given by

$$\frac{\partial^2 A_z}{\partial x^2} + \frac{\partial^2 A_z}{\partial y^2} - j\omega\mu_i\sigma_i A_z = 0 \tag{1}$$

where A_z is the magnetic vector potential, and μ_i and σ_i denotes the permeability and conductivity of each layer, respectively. The angular velocity ω is equal to $2\pi kf$, k and f is the time order and supply frequency, respectively. It is assumed that the magnet and shaft region have uniform permeability and conductivity, and the stator has zero conductivity, since it is laminated.

The general solution of (1) can be written as

$$A_{zi} = (C_i e^{\gamma y} + D_i e^{-\gamma y})e^{j(\omega t + \beta x)} \tag{2}$$

where γ is defined as

$$\gamma = \sqrt{\beta^2 + j\omega\mu_i\sigma_i} \tag{3}$$

where $\beta = \pi/\tau$, τ is the pole pitch.

Neglecting end effect, the tangential and normal flux density in a particular layer can be obtained as follows

$$B_{xi} = \frac{\partial A_{zi}}{\partial y} = \gamma(C_i e^{\gamma y} - D_i e^{-\gamma y})e^{j(\omega t + \beta x)} \tag{4}$$

$$B_{yi} = -\frac{\partial A_{zi}}{\partial x} = -j\beta(C_i e^{\gamma y} + D_i e^{-\gamma y})e^{j(\omega t + \beta x)} \tag{5}$$

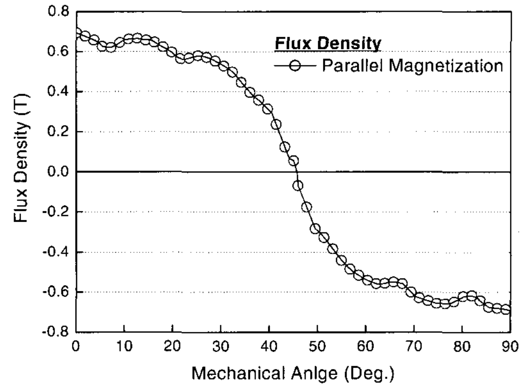

Fig. 6 Space distribution of the normal flux density over the sleeve surface of the parallel magnetized rotor. (Initial position)

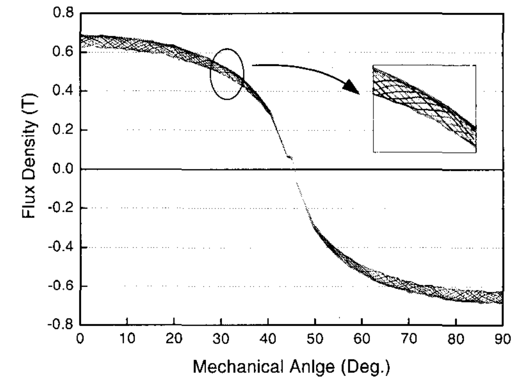

Fig. 7 Space distribution of the normal flux density over the sleeve surface parallel magnetized rotor. (15-data according to rotor angular position)

Table 2 Flux Harmonics of Parallel Magnetization

Space Order	Time Order		
	0	12	24
1	0.762456	0.000073	0.000117
3	0.133681	0.000207	0.000126
5	0.050400	0.000505	0.000039
7	0.023075	0.001208	0.000082
9	0.011434	0.003730	0.000039
11	0.005485	0.016166	0.000110
13	0.002422	0.018064	0.000141
23	0.002471	0.000103	0.004178
25	0.002430	0.000327	0.004916

The parameters C_i and D_i are calculated for each layer by boundary conditions, that is, interlayer field continuity requirements. The field equation is set as in the following matrix form.

$$\mathbf{A\,x = J}$$
$$\mathbf{x} = [D_1, C_2, D_2, C_3, D_3, C_4, D_4, C_5]^t$$
$$\mathbf{J} = [0, 0, 0, 0, 0, 0, 0, J_m]^t \quad (6)$$

where, **A** is the coefficients matrix and **J** is the current sheet, which is assumed to vary sinusoidally in both space and time and to flow in the axial direction of the machine. It can be described as follows

$$J(z) = J_m \cos(\omega t + \beta x) \quad (7)$$

For each region, to be designated by suffix, the electric field intensity may be expressed in terms of the magnetic vector potential as

$$E_{zi} = -\frac{\partial A_{zi}}{\partial t} = -j\omega(C_i e^{\gamma y} + D_e e^{-\gamma y})e^{j(\omega t+\beta x)} \quad (8)$$

3. Rotor Loss Analysis

The Poynting vector is a powerful means of obtaining the total power entering or leaving a region [6]. The Poynting vector, P, is defined in terms of the vector product of the electric field intensity and the magnetic field intensity over the surface of a region. For a sinusoidal electromagnetic field at steady-state, the average power transmitted through a surface is calculated using the Poynting vector in the following form

$$\mathbf{P = E \times H}$$
$$P = \frac{1}{2}\mathrm{Real}(E_z \times H_x^*) \quad (9)$$

where E_z is the amplitude of the electric field intensity in the axial direction and H_x^* is the amplitude of the conjugate of the tangential magnetic field intensity. Integrating (9) over the surface results in the total power transmitted through the surface [6].

Table 3 and Table 4 depict the rotor loss density under the no-load condition for a permanent magnet high-speed machine having a Halbach and parallel magnetized rotor, respectively. Rotor losses are mainly due to the principal time harmonic order 12th and space harmonic order 11th and 13th, as expected. Most of the rotor losses are in the conducting sleeve and magnets, also as expected.

Fig. 8 shows the comparison of rotor loss density for the time and space harmonics for permanent magnet rotor topologies. It can be seen that the Halbach magnetized rotor has a smaller total rotor loss density than the parallel magnetized rotor. The permanent magnet motor with Halbach magnetization has a lower total rotor loss density of about 88.4% than one with parallel magnetization.

Table 3 Rotor Loss Density for Halbach Magnetized Machine

Space Order	Time Order 0	12	24
1		0.1513	1.3157
3		0.6465	1.6576
11		152.3144	0.0098
13		84.0196	0.0073
23		0.0035	4.9367
25		0.0020	2.6677
Total Loss Density	237.5(12th)+10.8(24th) =248.3 W/m^2		

Table 4 Rotor Loss Density for Parallel Magnetized Machine

Space Order	Time Order 0	12	24
1		0.2412	0.8686
3		1.1681	1.1542
5		1.5834	0.0332
7		3.1989	0.0539
9		14.0281	0.0057
11		142.2009	0.0243
13		106.5613	0.0240
23		0.0041	3.7544
25		0.0048	4.0456
Total Loss Density	269.9(12th)+10.7(24th) =280.6 W/m^2		

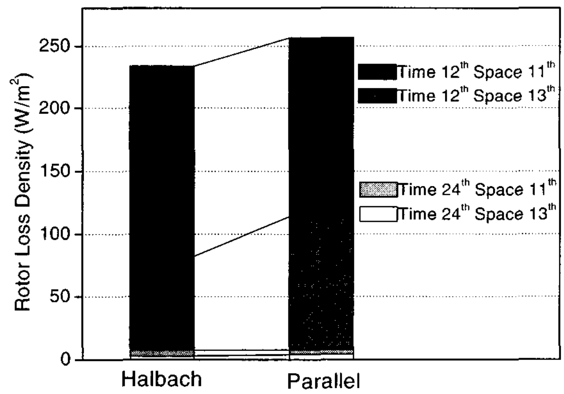

Fig. 8 Comparison of rotor loss density with time and space harmonic component.

4. Conclusion

The analytical field analysis and 2-D finite element method have been used to investigate the rotor eddy current losses of a permanent magnet high-speed machine with a Halbach or parallel magnetized rotor. A comparative study has shown that the permanent magnet machine with a Halbach magnetized rotor has lower rotor losses than the parallel magnetized one. The permanent magnet machine with Halbach magnetization topology is adapted to application of the high-speed device in order to reduce the rotor losses.

Table 5 Electric properties of rotor component

Item	Material	Resistivity
Retaining Sleeve	Titanium	177×10^{-8}
Permanent Magnet	N35H	130×10^{-8}
Shaft	Arnon7	15×10^{-8}

References

[1] K.Ng, Z.Q.Zhu and D.Howe, "Open-circuit field distribution in a brushless motor with diametrically magnetized PM rotor, accounting for slotting and eddy current effects," *IEEE Trans. Magn.*, vol.32, pp.5070-5072, Sept. 1997.

[2] Z.Q.Zhu, K.Ng and D.Howe, "Design and analysis of high-speed brushless permanent magnet motors," *Electrical Machines and Drives*, pp.381-385, Sept. 1997.

[3] Janne Nerg, Markku Niemelä, Juha Pyrhönen, Jarmo Partanen, "FEM calculation of rotor losses in a medium speed direct torque controlled PM synchronous motor at different load conditions," *IEEE Trans. Magn.*, vol.38, pp.5070-5072, Sept. 1997.

[4] S.M.Abu Sharkh, M.R. Harris, N.Taghizadeh Irenji, "Calculation of rotor eddy current loss in high-speed PM alternators," *Electrical Machines and Drives*, pp.170-174, Sept. 1997.

[5] S.M.Abu Sharkh, M.R. Harris, N.Taghizadeh Irenji, "Effect of power factor on rotor loss in high-speed PM alternators," *Electrical Machines and Drives*, pp.346-350, Sept. 1999.

[6] N. Taghizadeh Irenji, "Calculation of rotor electromagnetic losses in high-speed permanent magnet machines," Ph.D. dissertation, Univ. of Southampton, UK, 1998.

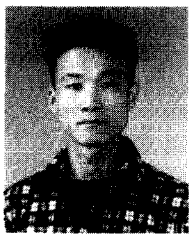

Han-Wook Cho

He was born in Korea in 1976. He received his B.S. and M.S. degrees in Electrical Engineering from Chungnam National University in 2002 and 2004, respectively. He is currently working toward his Ph.D. in the Dept. of Electrical Engineering at Chungnam National University. His research interests include the design and analysis of permanent magnet high-speed machines.

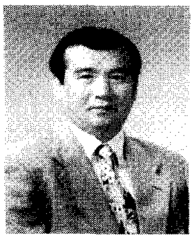

Seok-Myeong Jang

He was born in Korea in 1949. He received his B.E, M.S., and Ph.D. degrees from Hanyang University in 1976, 1978, and 1986, respectively. Currently, he is a Professor in the Department of Electrical Engineering at Chungnam National University. He worked as a Visiting Researcher in the Department of Electrical Engineering at Kentucky University in 1989. He is presently Vice President of KIEE and President of the EMECS Society. His field of interest includes the design and application of Linear Machines, Permanent Magnet Synchronous Machines, and Linear Oscillating Actuators.

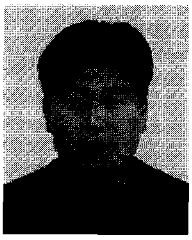

Sung-Ho Lee

He was born in Korea in 1971. He received his B.S., M.S. and Ph.D. degrees in Electrical Engineering from Chungnam National University in 1997, 1999 and 2003, respectively. His research interests include the design and analysis of permanent magnet machines and virtual instrumentation systems. He has also worked in the LG D/A Research Lab.

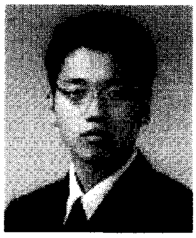

Hyun-Sup Yang

He was born in Korea in 1971. He received his B.S. and M.S. degrees in Electrical Engineering from Chungnam National University in 1998 and 2000, respectively. His research interests include design and analysis of permanent magnet high-speed machines. He has worked at SAMSUNG TECHWIN Co., LTD.

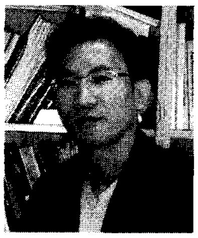

Yeon-Ho Jeong

He was born in Korea in 1968. He received his B.S. and M.S. degrees in Electrical Engineering from Chungnam National University in 1993 and 1996, respectively. He is currently working toward his Ph.D. in the Department of Electrical Engineering at Chungnam National University. He has also previously worked for KERI, as part of the Mechatronics Group.